NOAA Technical Memorandum NMFS-AFSC-510

Abundance and Distribution of Eastern Bering Sea Belugas from 2024 Aerial Line-Transect Surveys

P. B. Conn, K. E. W. Shelden, A. A. Brower, C. L. Christman, and K. T. Goetz

February 2026

U.S. DEPARTMENT OF COMMERCE

National Oceanic and Atmospheric Administration
National Marine Fisheries Service
Alaska Fisheries Science Center

The National Marine Fisheries Service's Alaska Fisheries Science Center uses the NOAA Technical Memorandum series to issue informal scientific and technical publications when complete formal review and editorial processing are not appropriate or feasible. Documents within this series reflect sound professional work and may be referenced in the formal scientific and technical literature.

The NMFS-AFSC Technical Memorandum series of the Alaska Fisheries Science Center continues the NMFS-F/NWC series established in 1970 by the Northwest Fisheries Center. The NMFS-NWFSC series is currently used by the Northwest Fisheries Science Center.

This document should be cited as follows:

Conn, P. B., Shelden, K. E. W., Brower, A. A., Christman, C. L., and Goetz, K. T. 2026. Abundance and distribution of eastern Bering Sea belugas from 2024 aerial line-transect surveys U.S. Department of Commerce, NOAA Technical Memorandum NMFS-AFSC-510, 35 p.

This document is available online at:

Document available: https://repository.library.noaa.gov

NOAA FISHERIES

Abundance and Distribution of Eastern Bering Sea Belugas from 2024 Aerial Line-Transect Surveys

P. B. Conn[1], K. E. W. Shelden[1], A. A. Brower[1], C. L. Christman[2], and K. T. Goetz[1]

[1]Marine Mammal Laboratory
National Marine Fisheries Service, NOAA
Alaska Fisheries Science Center
7600 Sand Point Way NE
Seattle, WA 98115

[2]Cooperative Institute for Climate, Ocean & Ecosystem Studies
University of Washington
3737 Brooklyn Ave NE
Seattle, WA 98105

U.S. DEPARTMENT OF COMMERCE

National Oceanic and Atmospheric Administration
National Marine Fisheries Service
Alaska Fisheries Science Center

NOAA Technical Memorandum NMFS-TM-AFSC-510

February 2026

ABSTRACT

In 2024, we conducted an aerial line-transect survey of the Eastern Bering Sea (EBS) stock of beluga whales (*Delphinapterus leucas*) in Alaska, USA. In this survey, a team of observers scanned for marine mammals from bubble windows installed on an Aero Commander aircraft, which flew pre-planned transects. Observers recorded sightings of beluga groups, location of beluga sightings (including perpendicular distance from the aircraft), and environmental conditions thought to influence detection (e.g., turbidity, Beaufort Scale sea state). We estimated perception bias using multi-covariate distance-sampling detection models and used resultant estimates to fit spatially-explicit density surface models (DSMs) to beluga sightings. These models included corrections for availability and imperfect detection on the transect line obtained from independent sources. Our fitted models predicted high beluga densities north of Pastol Bay, Alaska, and in turbid waters near the Yukon River Delta. However, there was considerable sensitivity relative to inclusion of two "supergroups" of 277 and ≈ 500 belugas detected near Scammon Bay, Alaska. The size of these supergroups was far above the normal range of group sizes encountered during this survey (range: 1-38; mean 3). These supergroups were also encountered outside of normal transect effort. We considered several approaches for accounting for these groups, including (1) ignoring them; (2) treating supergroups as an additional class of whales with 100% detection (though with incomplete availability); and (3) treating them as having been detected while "on effort" (option 3 was primarily used for sensitivity analysis). Resultant ensemble estimates of abundance from DSMs were $\widehat{N} = 6{,}360$ (CV 0.16), $\widehat{N} = 7{,}917$ (CV 0.13), and $\widehat{N} = 10{,}425$ (CV 0.25), respectively. Of these estimates, we consider $\widehat{N} = 7{,}917$ (CV 0.13) to be the most

defensible from a statistical perspective; however, we caution that there is considerably more uncertainty than indicated by the low CV. In addition to uncertainty relative to supergroups, we also encountered a pod of killer whales (*Orcinus orca*) during the survey that may have altered the spatial distribution of belugas while the survey was being conducted. For these reasons, we recommend that contemporary management of the EBS stock be based on a previous estimate from the 2022 surveys (Ferguson et al. 2025), $\widehat{N} = 13{,}313$ (CV 0.22). Contemporary distance sampling methods seem ill equipped to handle supergroups or large-scale changes in whale distribution while surveys are being conducted. We recommend further research in survey methodology before the next survey of this stock is conducted.

CONTENTS

INTRODUCTION

The Eastern Bering Sea stock (EBS) of beluga whales (*Delphinapterus leucas*) is one of four genetically distinct western Alaska beluga stocks (O'Corry-Crowe et al. 1997), each of which is co-managed by the Alaska Beluga Whale Committee and U.S. National Marine Fisheries Service (Adams et al. 1993, Frost et al. 2021). The EBS stock reliably inhabits Norton Sound, Alaska, and portions of the Yukon River Delta during ice-free months (typically late-May to November; Citta et al. 2017, Lowry et al. 2017) and is an important cultural and subsistence resource to Alaska Native communities in the region. Accurate estimates of abundance and distribution are important for assessing the stock and for ensuring the sustainability of beluga harvests for future generations.

To update abundance estimates, we conducted an aerial line-transect survey of the EBS stock over a two-week period (18 June – 1 July) in the summer of 2024. An in-depth summary of the data and field effort has previously been published (Shelden et al. 2024). The purpose of the present document is to use recently developed spatial models for survey data (Ferguson et al. 2025) to estimate abundance and produce maps of spatial distribution. These models are versions of density surface models (DSMs; Miller et al. 2013) but use location (rather than environmental covariates) to predict spatial distribution.

The remainder of this report is structured as follows. First, we review basics of the study area, survey design, and field collection methods. Second, we describe the inferential framework that we used for estimation, uncertainty propagation, and sensitivity analyses. After presenting results from different models and sets of assumptions, we close with a discussion of ways that surveys can be improved in the future, specifically in regard to

increasing observations of large aggregations of whales (i.e., “supergroups”) in EBS surveys, and to the presence of killer whales (*Orcinus orca*) in the survey area. Both factors made straightforward interpretation of EBS beluga estimates challenging for the 2024 survey.

METHODS

Study Area

Our study area consisted of the ocean waters of Norton Sound, Alaska, together with adjacent waters off the Yukon River Delta (Fig. 1). The Yukon River Delta is characterized by highly turbid waters, which is evident by examining satellite imagery of the region (Fig.1). This study area represents a gradual evolution in monitoring the EBS stock. In particular, the most recent survey in 2022 (Ferguson et al. 2025) extended the surveyed area farther south from what had been surveyed in 2000 and 2017 surveys (Lowry et al. 2017, Ferguson et al. 2023).

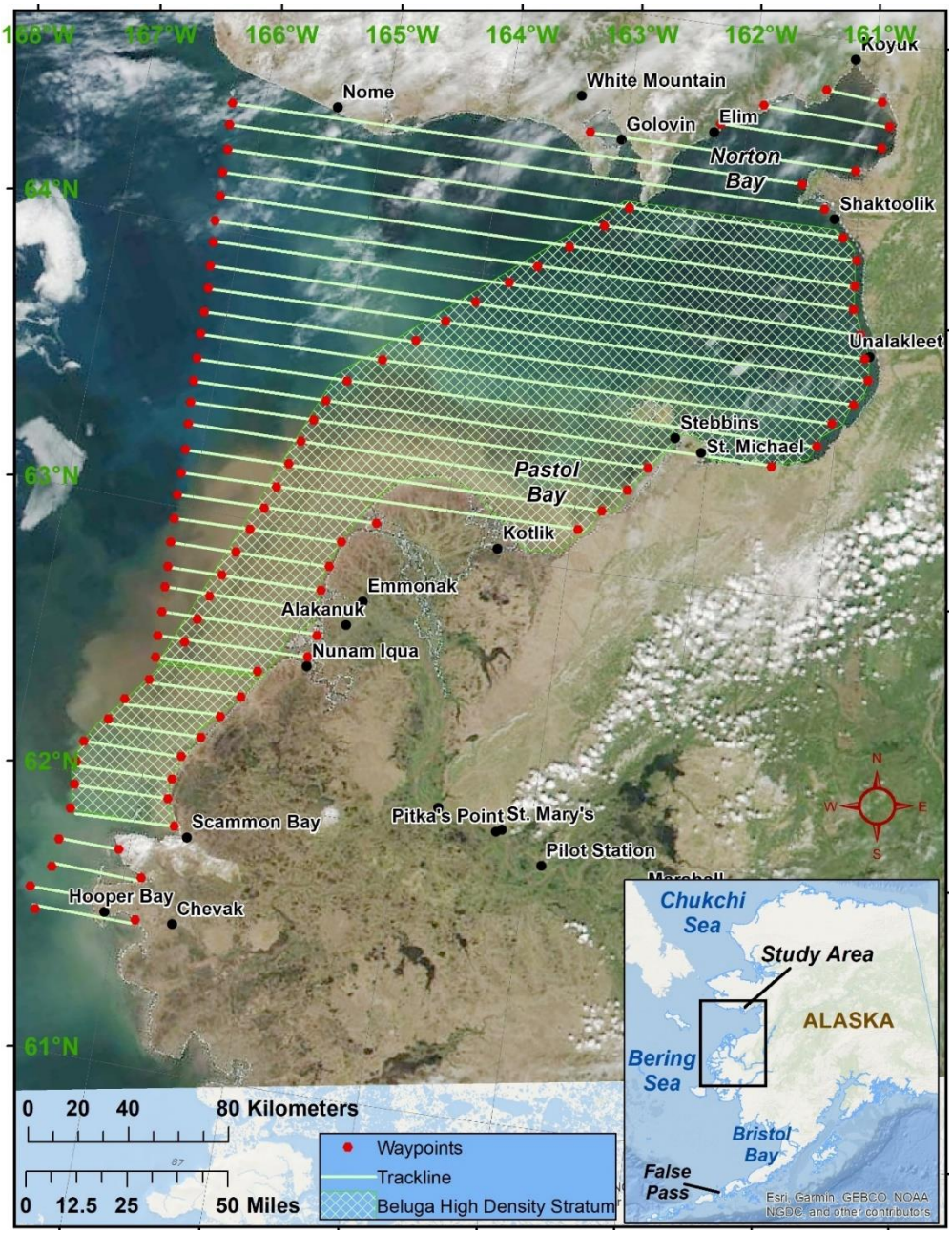

Fig. 1. -- Study area and planned aerial transects for the 2024 eastern Bering Sea beluga survey. The cross-hatched area represents a "high density" stratum, some of which received increased effort. The background image was a MODIS product from 16 June 2024 (https://worldview.earthdata.nasa.gov). Figure reproduced from Shelden et al. (2024).

Aerial Line-Transect Methods

An in-depth description of line-transect survey methods and raw data are provided in a previously published report (Shelden et al. 2024). However, for completeness, we review the basic details here (some of this description is reproduced from the Shelden et al. 2024 report).

Line-transects were oriented east-west and were spaced 9.3 km (5 nmi) apart, with the initial position determined by a random starting point (consistent with systematic random sampling), covering the full study area (Fig. 1). Transect lengths ranged from 22 to 267 km. As in the 2022 survey, the southern end of the study area included transects near Scammon Bay, Alaska (note that earlier surveys, such as in 2017, did not include effort this far south). One notable departure from previous designs was inclusion of a "high density" stratum that was targeted for repeat efforts when weather permitted (Fig. 1). The total study area was 46,898 km^2.

Transects were flown with a Turbo Commander aircraft from 18 June to 1 July 2024 with a target altitude of 320 m and a target speed of 213 km/h. Each flight had both left- and right-side observers as well as a data recorder. Each observer made observations through bubble windows, providing unobstructed views around the aircraft. Scanning was with the naked eye, with binoculars only used for verification and magnification of detected beluga groups. Declination angles from the horizon to each sighting were measured using handheld clinometers when the sighting was abeam and were used to calculate perpendicular distance from the transect line. Each "sighting" or "group" was defined as all animals within five body lengths of each other. In this context, we consider groups of whales to be the primary sampling unit. In a few cases where there were large groups that

were more dispersed, observers kept track of a running total and these were treated as a single group and an average declination angle was used. In some of these cases, the aircraft broke off from the survey line to obtain a more accurate count (i.e., "closing mode") before resuming transect effort.

In addition to beluga sightings, observers also recorded covariates thought to influence detection. These included weather conditions (e.g., Beaufort Scale sea state) and environmental conditions (e.g., water turbidity). Prior to analysis, data were filtered to only include effort and sightings obtained in Beaufort Scale sea state 4 or less.

Statistical Analysis

Overview

In order to generate abundance estimates from our survey data, we employed two conceptually different estimation procedures. Our primary mode of inference was to fit spatially-explicit density surface models (DSMs; Hedley and Buckland 2004, Miller et al. 2013) to counts of belugas made during our surveys. In this case, model-based predictions of beluga abundance are summed across the survey area to provide an overall abundance estimate. This was the approach taken by Ferguson et al. (2025) for use with 2017 and 2022 surveys and was accepted by the Alaska Scientific Review Group as the preferred estimate of abundance for these years (meeting 4 March 2025, NOAA, Alaska Fisheries Science Center, Seattle, WA).

Our secondary mode of inference was a stratified design-based procedure, which has historically been used for EBS beluga abundance estimation (e.g., Lowry et al. 2017, Ferguson et al. 2023). However, unlike DSMs, this approach does not generate detailed

maps of beluga density, nor does it cope well with deviations from preplanned survey tracks (e.g., due to weather) or when there is duplicated effort, both of which occurred during 2024 surveys. As such, we view the stratified design-based estimates as more of a "ground check" on DSM estimates, as well as an effort to maintain historical continuity.

Under both approaches to inference, a detection function was first fit to distance data (as in Buckland et al. 2001) and combined with availability probability and transect detection probability (i.e., *g(0)* in distance sampling terminology) to produce a cumulative detection estimate. As such, we first describe detection modeling. We then proceed to describe DSM and design-based procedures, as well as the general approaches that we used for error propagation and model checking.

Detection modeling

We model cumulative detection probability as a function of three conceptually distinct components: (i) detectability on the transect line, conditional on belugas being available to be detected, $g(0; \boldsymbol{z}_i)$; (ii) detectability of available whales as a function of perpendicular distance *d* from the transect line, $p_{ds}(d; \boldsymbol{z}_i)$, and (iii) availability of whales (i.e., the probability that a whale is at the surface sometime within the duration it takes the aircraft to pass overhead; Marsh and Sinclair 1989), $a(\boldsymbol{z}_i)$. Each of the three components of detection is possibly dependent on a vector of covariates associated with whale group *i*, denoted by $\boldsymbol{z}_i$. The cumulative detection function, *p*, can then be written as

$$p(d; \boldsymbol{z}_i) = g(0; \boldsymbol{z}_i) p_{ds}(d; \boldsymbol{z}_i) a(\boldsymbol{z}_i).$$

Essentially, the distance sampling component $p_{ds}(d; \boldsymbol{z}_i)$ governs how detection decreases with distance from the transect line, while $g(0; \boldsymbol{z}_i)a(\boldsymbol{z}_i)$ determines the y-intercept of the cumulative detection function.

Ferguson et al. (2023, 2025) based $g(0; \boldsymbol{z}_i)$ on a double-observer study conducted during surveys of belugas in the Chukchi and Beaufort seas in 2018 and 2019 (Clarke et al. 2019, 2020). This study used time stamps of images of belugas from a downward-facing camera together with human-based real time detections to construct a mark-recapture estimate of detection probability. Using this approach, they obtained an overall transect detection probability of 0.753 (CV 0.015). Although a downward facing camera was also employed during the 2024 EBS survey, there were considerable impediments to reliable matching of photographs with human observations (Shelden et al. 2024); therefore, we use $\hat{g}(0; \boldsymbol{z}_i) = 0.753$ as in previous analyses of the EBS beluga stock.

We also follow Ferguson et al. (2023, 2025) in basing $a(\boldsymbol{z}_i)$ on a study of dive and surfacing intervals of three adult female Beaufort Sea belugas, together with an independent estimate of the viewing time that a beluga is in view of the Turbo Commander while passing overhead (McLaren 1961). Ferguson et al. (2023) calculated $\hat{a}(\boldsymbol{z}_i) = 0.499$, and in absence of an associated uncertainty estimate treated it as a fixed value. Although this estimate is only based on three whales located in a different region, it appears to be the only attempt that has been made to quantify surfacing behavior of Alaska belugas. Nevertheless, readers should treat resultant abundance estimates with caution, especially since uncertainty in availability probability cannot be reliably propagated into final abundance estimates.

For the distance-based detection function, $p_{ds}(d; \boldsymbol{z}_i)$, we used a standard multi-covariate distance sampling modeling framework (Marques and Buckland 2003) to estimate associated parameters. The 2024 EBS beluga survey employed three observers (CLC, KTG, and KEWS), and although all were experienced marine mammal observers, only one had participated in previous EBS beluga surveys (KEWS). Initial inspection of detection data suggested that there were different effective truncation distances in the 2024 survey relative to 2017 and 2022 surveys, so we fitted entirely new detection functions. In particular, the distribution of observed perpendicular distances for the 2024 survey had a mode of 225 m and a 95th quantile of 1,441 m. In contrast, 2017 and 2022 surveys had modes near 50 m and 75 m, respectively, and a 95th quantile near 1,000 m. It appears that observers in the 2024 survey tended to focus detections farther away from the aircraft than in previous surveys. For this analysis, we set the left truncation distance to 150 m and the right truncation distance to 1,441 m. The 150 m value seemed justified given the lack of detections prior to this value (Fig. 2).

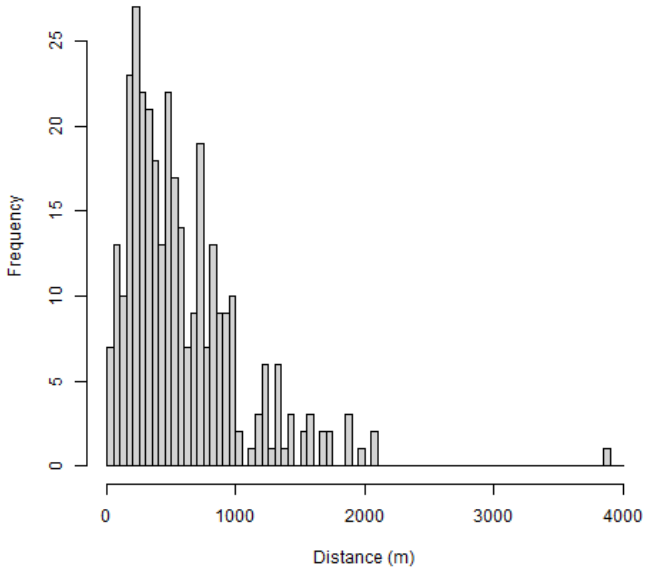

Fig. 2. -- Histogram of all observed perpendicular distances (km) from the transect line to observed beluga groups in the 2024 aerial survey.

We fitted a number of multi-covariate detection models (Marques and Buckland 2003) to our data and used model with the lowest AIC value for inference (Burnham and Anderson 2002). In particular, we considered models that included all factorial combinations of covariates listed in Table 1, together with two types of detection functions: half-normal and hazard rate (Buckland et al. 2001). We fitted detection models to our data in the R programming environment (R Core Team 2024), specifically using the `mcds` function within the `mrds` package (Laake et al. 2024). We then proceeded with the highest ranked detection model for subsequent analyses (Fig. 3).

Table 1. -- Covariates used in distance sampling analyses of 2024 Eastern Bering Sea belugas.

Covariate	Parameterization(s)
Group size	*catsize* (factor; 1, 2+) *catsize3* (factor; 1, 2, 3+) *catsize10* (factor; 1,2-9,10+) *catsize10b* (factor: 1-9,10+) *loggs* (continuous on log scale)
Turbidity	*turb* (binary)
Beaufort Scale sea state	*iBeauf* (factor; 2,3,4) *cBeauf* (continuous)

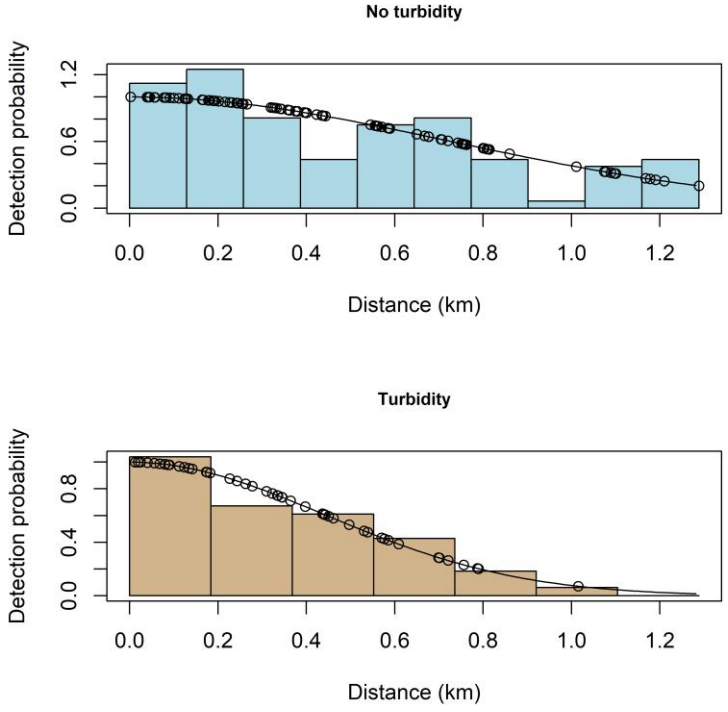

Fig. 3. -- Histograms of observed perpendicular distances (km) from the transect line to observed beluga groups in the 2024 aerial survey, together with fitted half-normal detection functions (solid black line) and actual observed distances (open black circles). Detection functions decreased faster in turbid waters than non-turbid waters, indicating poorer detection. Note that distances plotted here incorporate a left truncation distance of 150 m, such that a distance of 0.0 in the plot corresponds to 150 m away from the aircraft.

Density surface models (DSMs)

In a second step, cumulative detection estimates were used as a log-offset in a generalized linear mixed model framework to explain variation in beluga counts obtained over 10 km transect segments. As explained by Miller et al. (2013), segments should be short enough that there is little change in expected density within a segment, and we selected 10 km as a reasonable level of spatial resolution given this guideline. Transect segments were formed by splitting "on effort" transect lines into 10 km segments, with any segments <10 km long joined back together with the nearest 10 km segment, as in Ferguson et al. (2025). Any survey effort conducted in Beaufort Scale sea state 5 or 6 was also omitted, and counts were restricted to belugas with perpendicular distances from the transect line between 150 and 1,441 m. Figure 4 shows segment centroids and beluga counts associated with each segment.

For continuity in estimation, we use the same overall model structure as in previous analyses of 2017and 2022 survey data (Ferguson et al. 2025). Specifically, letting C_i denote the count of belugas made during aerial surveys of transect segment *i*, we model

$C_i \sim \text{Tweedie}(\mu_i, \phi, \rho)$,

where μ_i gives an expected count, and ϕ and ρ are dispersion and power parameters of the Tweedie distribution, respectively. Note that the Tweedie distribution requires $\phi > 0$, and we enforce the constraint $1 < \rho < 2$ (cf. Dunn and Smyth 2005, Sigourney et al. 2020). This version of the Tweedie distribution allows for overdispersion as well as zero inflation, two common features of ecological count data.

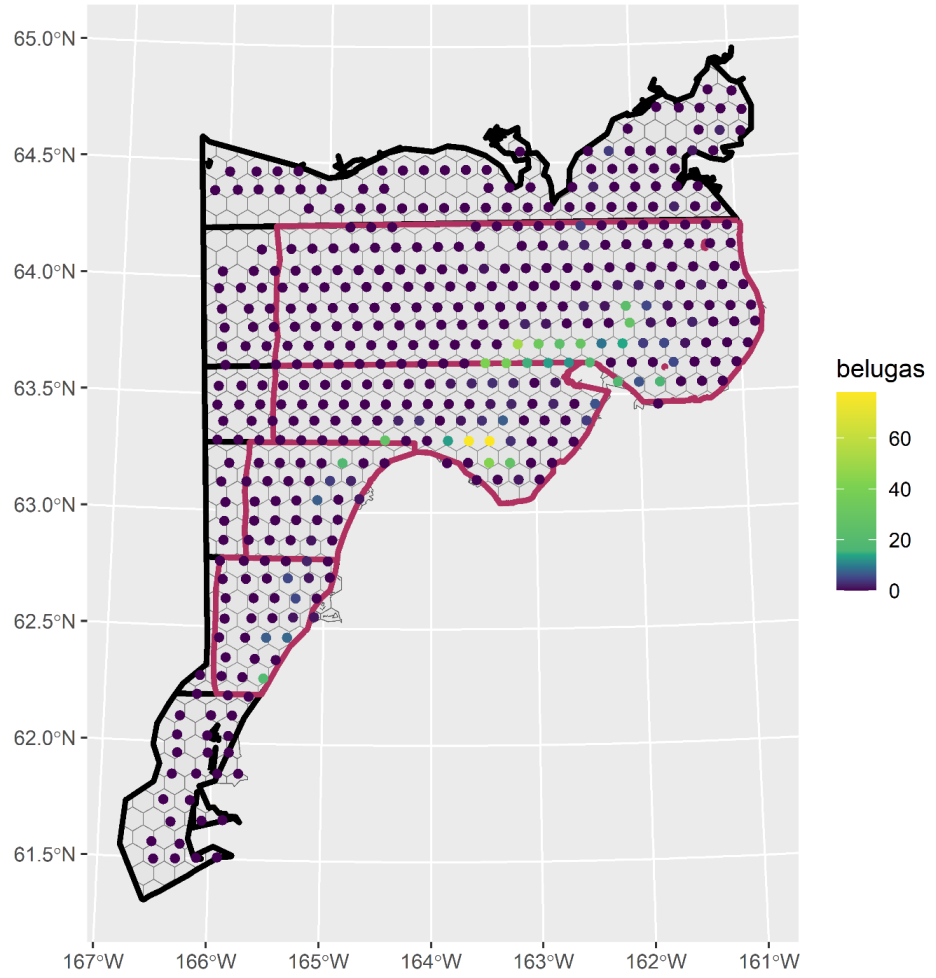

Fig. 4. -- Location of "on effort" line-transect segment centroids together with counts of belugas obtained between 150 m and 1,441 m in each segment (colored points). Also shown are the grid cells used for abundance predictions (hexagons), the six strata boundaries used for the design-based estimate in this study (black lines), and the four historical strata boundaries (maroon lines) used in analysis of survey data collected during the 2000 (Lowry et al. 2017) and 2017 (Ferguson et al. 2025) surveys. By contrast, the 2022 survey was conducted over the full survey area shown here (Ferguson et al. 2025). Note that maroon lines completely mask some of the black lines.

Further structure on μ_i allows us to model variation in abundance over space and to account for incomplete detection. Specifically, we model

$$\mu_i = a_i p_i \exp(\beta_0 + \delta_i).$$

Here, a_i gives the area surveyed in transect segment i ($i \in 1,2,\cdots,n_i$), p_i gives the cumulative detection probability (see previous section), β_0 represents an intercept parameter, and δ_i gives a spatially autocorrelated random effect associated with transect segment i. The spatial process is actually modeled at a set of n_η locations, $\boldsymbol{s}_\eta$ (also called "knots"), each with a random effect η_j. Spatial autocorrelation is induced by assuming that this vector of random effects is drawn from a mean-zero multivariate normal distribution with a spatially colored covariance matrix:

$\boldsymbol{\eta} \sim$ Multivariate normal$(\mathbf{0}, \boldsymbol{\Sigma})$.

The relationship between $\boldsymbol{\eta}$ and $\boldsymbol{\delta}$ is simply $\boldsymbol{\delta} = \mathbf{A}\boldsymbol{\eta}$, where $\mathbf{A}$ is an $(n_i \times n_\eta)$ interpolation matrix.

Like Ferguson et al. (2025), we work with the precision matrix $\mathbf{Q} = \boldsymbol{\Sigma}^{-1}$ rather than the variance-covariance matrix as it allows us to increase computational efficiency via sparse matrix routines. In particular, different ways of specifying $\mathbf{Q}$ correspond to different spatial models, including a stochastic partial differential equation (SPDE) approximation to the Matérn covariance function (Lindgren et al. 2011), an SPDE model incorporating barriers (Bakka et al. 2019), tensor products bases (Wood 2017), thin plate splines (Wood 2003), and soap film smoothing (Wood et al. 2008, Miller and Wood 2014). For technical details on computing $\mathbf{Q}$ for these models, the parameters of $\mathbf{Q}$ that need to be estimated, as well as ways of specifying $\mathbf{A}$, see Ferguson et al. (2025).

As in Ferguson et al. (2025), model fitting was conducted using Template Model Builder (TMB; Kristensen et al. 2015) within the R computing environment (R Core Team 2024). This framework also allowed us to compute abundance estimates for the entire survey area and associated standard errors. This was accomplished by predicting

abundance over a finite partition of our study area (in particular to a hexagonal grid) and then summing abundance across grid cells (Fig. 4). We fit the same set of spatial models to our data as in Ferguson et al. (2025), and similarly computed a single ensemble abundance estimate, $\widehat{N}$, as a simple average of the model-specific estimates. We also calculated an estimate restricted to the grid cells whose centroids were within the original Lowry et al. (2017) strata for historical comparison.

Variance is complicated by the fact that DSMs commonly employ a two-step procedure, whereby detection probability is first estimated and then treated as fixed when fitting the DSM. In order to propagate uncertainty about detection into the final estimates, extra work is needed. We follow Ferguson et al. (2025) in calculating variance for each model using the law of total variance. This procedure is further outlined in Conn and Ferguson (in review), who demonstrated it to have reasonable coverage properties in simulation studies.

We assessed the fit of our models by examining diagnostics generated through the DHARMa package (Hartig 2022) in R. In particular, we examined quantile-quantile plots and plots of probability integral transform (PIT) residuals.

Stratified, design-based estimate

We used the `dht` function from the mrds library in R to produce a design-based abundance estimator. The `dht` function uses a Horvitz-Thompson-like estimator for each strata *k*, such that the abundance estimate for strata *k* is

$$\widehat{N_k} = \frac{A_k}{a_k} \sum_{g=1}^{n_k} s_g / p_g.$$

Here, A_k gives the total area of strata k, a_k gives the total on-effort area surveyed in strata k (the width of transects is taken to be the distance between left and right truncation endpoints), n_k gives the total number of beluga groups encountered within transect boundaries while on effort in strata k, s_g gives the number of belugas in the gth beluga group, and p_g gives cumulative detection probability for group g. The total abundance estimate (across strata) is then simply

$\widehat{N} = \sum_k \widehat{N_k}$.

We produced two such estimates: one corresponding to the original four strata used by Lowry et al. (2017) and another using the six strata employed by Ferguson et al. (2025) (Fig. 4).

Sensitivity to missed "supergroups"

We also conducted a sensitivity analysis to see what would happen to DSM estimates had two supergroups of belugas (277 and ≈ 500 individuals, respectively; Fig. 5) been observed within the transect strip while on effort (we set detection probability to 1.0 for these groups). One of these groups (277) was detected off effort, while another was detected at a range of ≈ 3 km away from the transect line and was censored after establishing a right truncation distance close to 1.5 km. In both cases, we associated these supergroups with the closest transect segment when conducting the sensitivity analysis. We also produced an alternative estimator that assumes that supergroups within the study area have 100% detection, effectively adding supergroup abundance to the DSM estimate after correcting the supergroup count for availability bias.

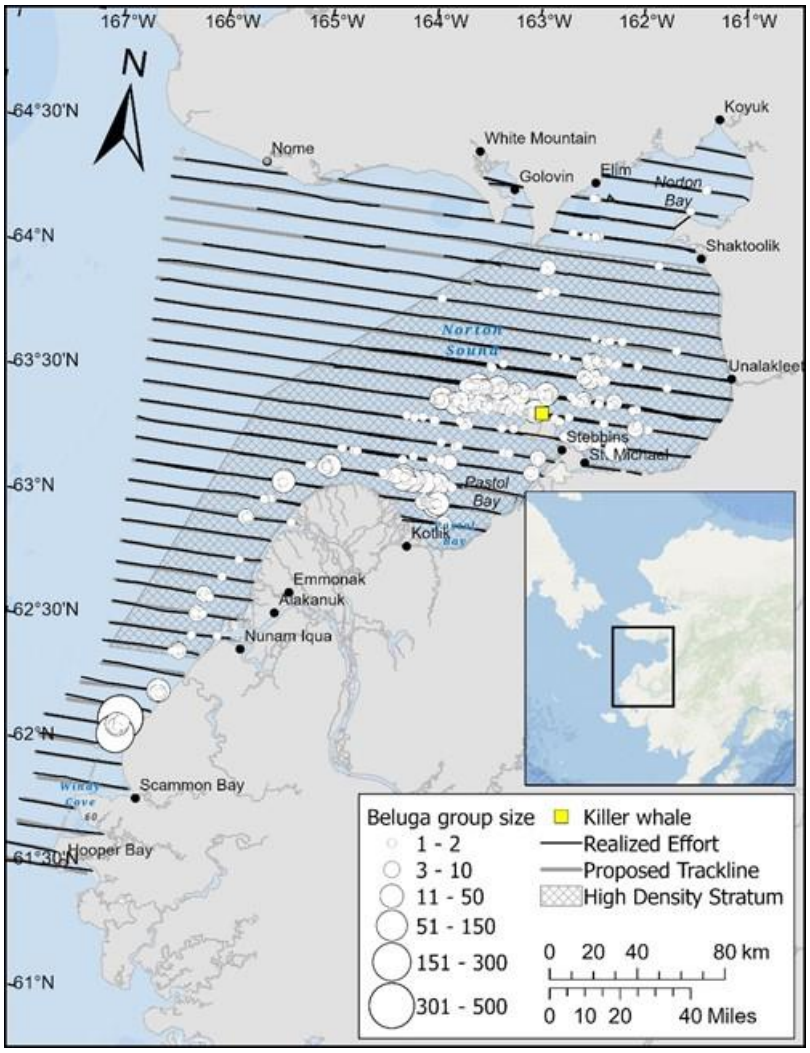

Fig. 5. -- Planned and realized transects together with the approximate location of individual beluga and killer whale sightings (both on and off effort). Note that the two largest sightings north of Scammon Bay (277 and ≈ 500 individuals, respectively) were not included in primary estimation models because they either occurred off effort or beyond the right truncation distance. These two observations were included in a sensitivity analysis, however. Figure adapted from Shelden et al. (2024).

RESULTS

General Data Summary

Over 7 survey flights between 18 June and 1 July, we conducted 6,934 km of transect effort. We sighted a total of 328 beluga groups consisting of 1,195 belugas while on transect, though this number was reduced to 277 groups totaling 832 belugas after filtering (primarily due to truncation distances). Observers found two "supergroups" of 277 and ≈ 500 belugas in the study area, both north of Scammon Bay, Alaska (Fig. 5). One of these groups was detected when on effort but out of the distance truncation range; the other was observed when in closing mode (off effort). For a more complete description of field data, see Shelden et al. (2024).

Statistical Analysis

Models fitted to perpendicular distances of detected whale groups (Table 2) favored a half-normal detection function with turbidity as a predictor for log-scale standard deviation (Fig. 3). Several other top models (ΔAIC within 2 units) included group size (with several different parameterizations) or Beaufort Scale sea state, but the only consistent predictor was turbidity. As such, we proceeded with a half-normal, turbidity-based detection model for all model fitting exercises. Note that average detection probability was almost identical for each of the models, so we do not expect detect model selection uncertainty to have much impact on resultant estimates (Table 2).

Table 2. --Fitted detection models, ranked by ΔAIC, where "Type" gives the functional form of the distance function (hn: half-normal; hr: hazard rate), "Covariate model" specifies the covariates in the model, k gives the number of parameters, and $\hat{p}$ (CV) gives the average estimated detection probability within truncation limits (and associated coefficient-of-variation). For brevity, we only present models within 2.0 AIC units of the highest ranked model.

Type	Covariate model	k	ΔAIC	$\hat{p}$ (CV)
hn	*turb*	2	0.00	0.56 (0.07)
hn	*turb* + *catsize10b*	3	0.58	0.55 (0.07)
hn	*turb* + *loggs*	3	1.36	0.55 (0.07)
hn	*turb* + *cBeauf*	3	1.45	0.56 (0.07)
hn	*turb* + *catsize*	3	1.99	0.55 (0.08)

Density surface models fitted to transect counts all appeared to fit the data well based on `DHARMa` diagnostics and generated total abundance estimates ranging from 5,917 to 6,729 (Table 3) with an equal-weight ensemble average of $\widehat{N} = 6{,}360$ (CV 0.16). When restricted to the four original strata used in the Lowry et al. (2017) analysis of survey data in 2000, the ensemble estimate was reduced to $\widehat{N} = 6{,}227$ (CV 0.16). For reference, the Lowry et al. (2017) strata encompassed 28,946 km^2, or 62% of the total survey area for 2024 surveys. DSMs with different spatial basis functions produced similar overall patterns of density (Fig. 6). Design-based stratified estimates and associated CVs were higher, with $\widehat{N} = 10{,}966$ (CV 0.30) for the full study area. However, we note that the design-based estimator assumes that all locations within a stratum are equally likely to be sampled, while in practice cumulative aerial survey efforts were biased towards locations with high whale densities (Fig. 7). Unless accounted for (e.g., through effort modifications or flexible spatial models), this type of preferential sampling (Conn et al. 2017) will tend to result in positive bias.

Table 3. -- Estimates of EBS beluga abundance from DSMs fitted to 2024 survey data. Estimates are for the full survey area ($\widehat{N}$) or restricted to Lowry et al. (2017) strata ($\widehat{N}_{Lowry}$), and each have an accompanying coefficient of variation (CV). Estimates vary based on the form of the spatial basis function (Model) and number of random effects (n_{RE}), with the fits to count data quantified via a negative log likelihood (NLL).

Model	$\widehat{N}$	$\widehat{CV}(\widehat{N})$	$\widehat{N}_{Lowry}$	$\widehat{CV}(\widehat{N}_{Lowry})$	NLL	n_{RE}
thin plate	6,503	0.14	6,391	0.14	303.0	307
tensor	6,729	0.15	6,579	0.15	327.3	323
SPDE	5,977	0.16	5,851	0.16	342.6	310
SPDE bnd	5,917	0.16	5,800	0.16	341.4	310
soap	6,674	0.15	6,516	0.15	325.8	311

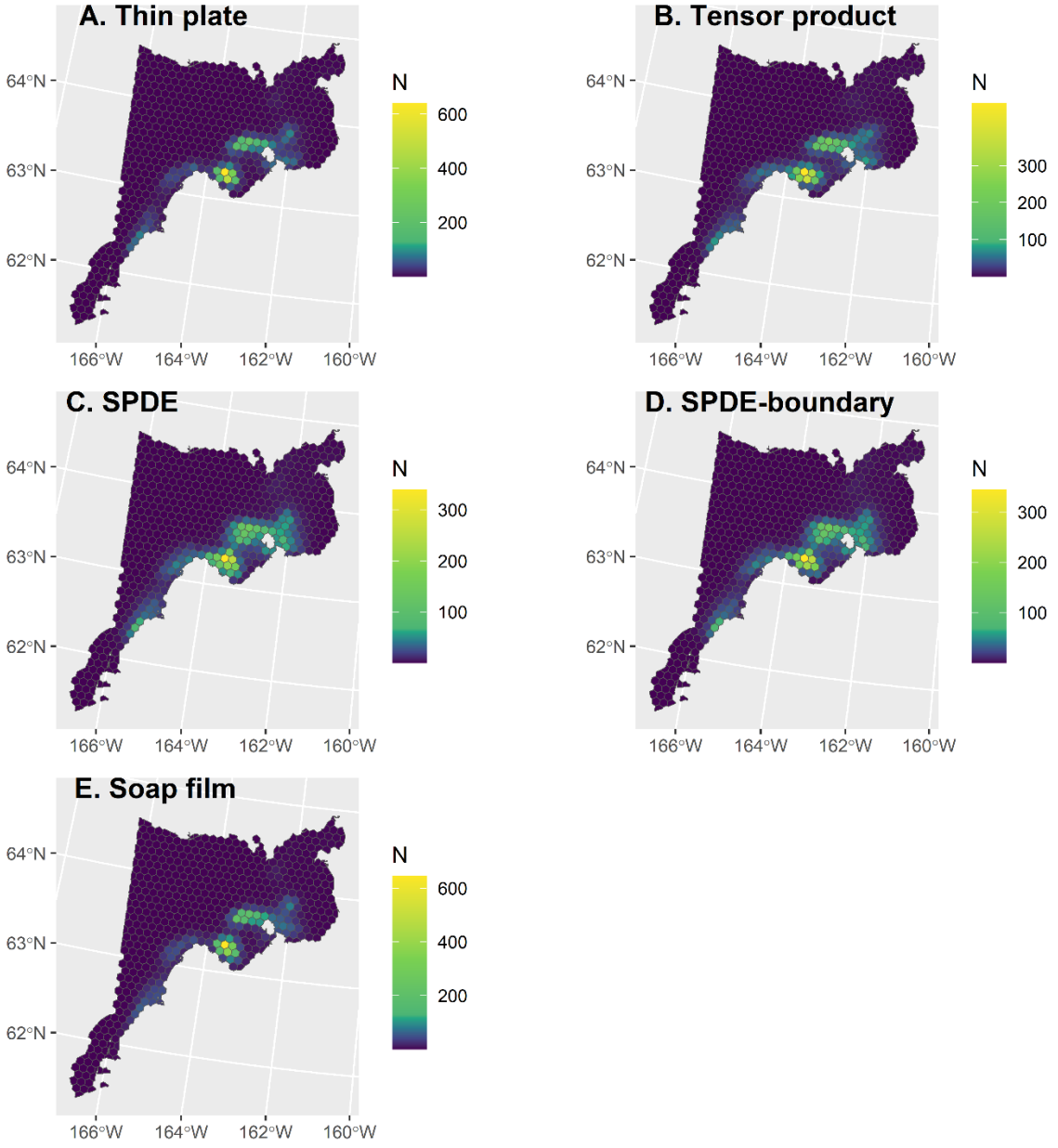

Fig. 6. -- Spatially-explicit estimates of abundance (N) for different density surface models fitted to 2024 aerial survey data of EBS belugas. Note that the color scale is slightly different for some of the models.

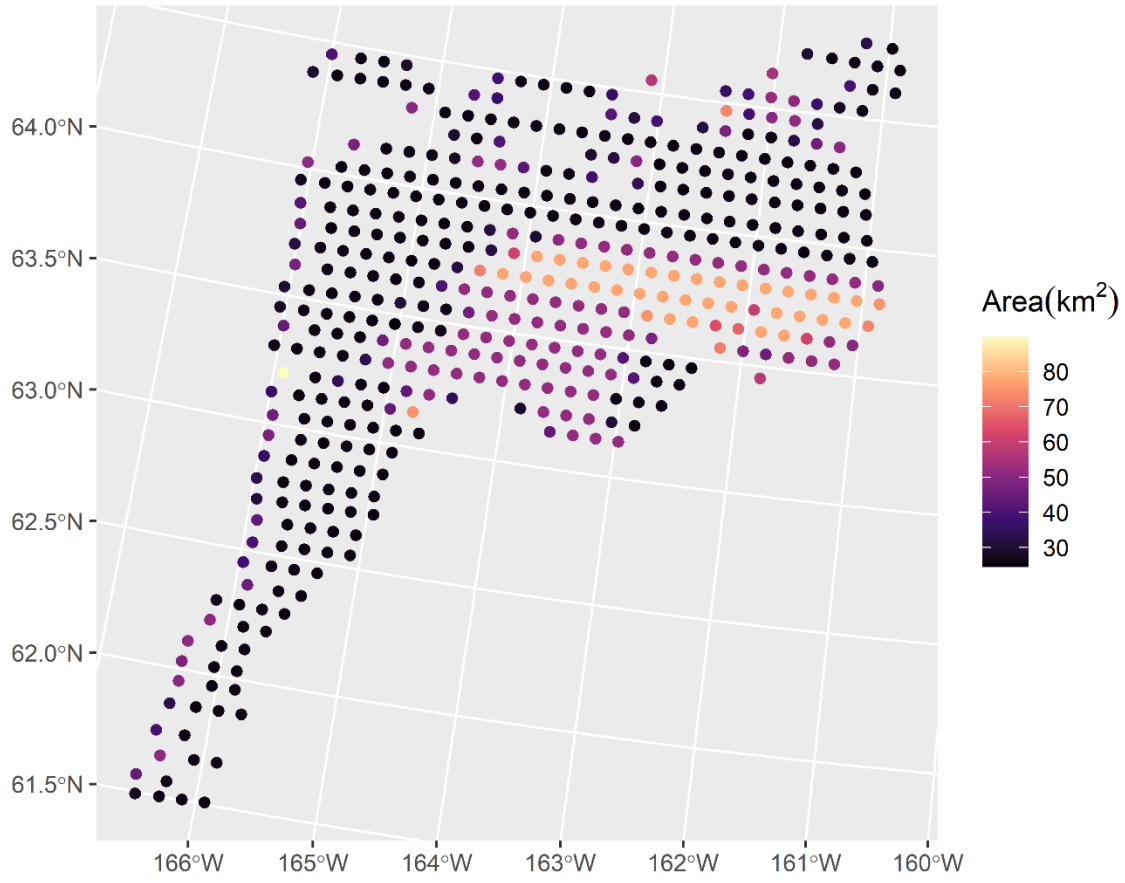

Fig. 7. -- Aerial survey effort (in km^2) for each of the 10-km transect segments used in the DSMs. Some of the transect segments were >10 km, but the primary reason for variation is that some of the segments were flown more than once. Many of the segments receiving duplicated effort were in areas where belugas were abundant, which can lead to positive bias (particularly for design-based estimators) unless accounted for explicitly.

We employed several approaches to account for two large "supergroups" not encountered while on survey effort within truncation boundaries. First, assuming all supergroups in the study area were detected, we simply added the implied abundance

associated with supergroups (after accounting for availability bias); calculated relative to the equal-weight ensemble, this approach results in an estimate of $\widehat{N} = 7{,}917$ (CV 0.13). As a second approach, we conducted a sensitivity analysis that reran each DSM, but included the two supergroups encountered near Scammon Bay, Alaska, as if they had been seen within the truncation range while on effort. In this case, estimates ranged from 7,842 to 13,042 with an ensemble average of 10,425 (CV 0.25) (Table 4). Differences in estimates were largely attributable to how many whales were predicted to be in the vicinity of Scammon Bay (Fig. 8).

Table 4. -- Estimates of EBS beluga abundance from sensitivity runs that treated two "supergroups" as if they had been detected while surveying "on effort." Estimates are for the full survey area ($\widehat{N}$) or restricted to Lowry et al. (2017) strata ($\widehat{N}_{Lowry}$), and each have an accompanying coefficient of variation (CV). Estimates vary based on the spatial basis function (Model) and number of random effects (n_{RE}), with the fits to count data quantified via a negative log likelihood (NLL).

Model	$\widehat{N}$	$\widehat{CV}(\widehat{N})$	$\widehat{N}_{Lowry}$	$\widehat{CV}(\widehat{N}_{Lowry})$	NLL	n_{RE}
thin plate	11,450	0.14	6,556	0.12	298.6	307
tensor	13,042	0.19	7,147	0.17	345.1	323
SPDE	8,266	0.16	5,876	0.16	344.2	310
SPDE bnd	7,842	0.15	5,825	0.16	345.3	310
soap	11,524	0.19	7,093	0.19	350.2	311

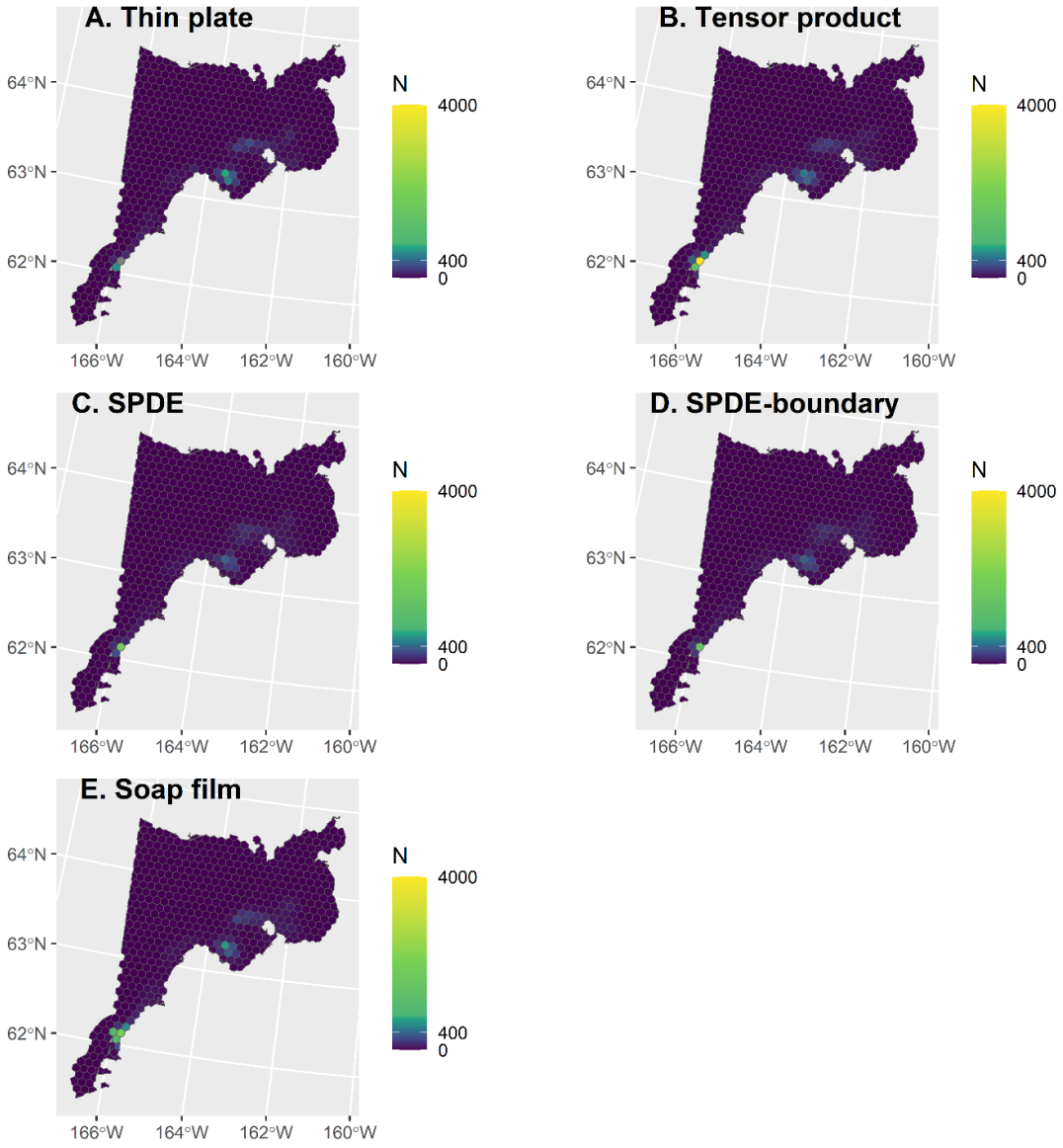

Fig. 8. -- Spatially-explicit estimates of EBS beluga abundance (*N*) for sensitivity runs that treated supergroups as if they were observed within transect boundaries while on effort. Due to extremely high predictions near Scammon Bay, Alaska, only cells with high abundance predictions are visible.

DISCUSSION

In this study, we employed an ensemble approach with density surface models to estimate the abundance of EBS belugas from 2024 aerial line-transect survey data. This strategy (and the particular models that were implemented) was purposefully duplicated from previous analyses of 2017 and 2022 survey data (Ferguson et al. 2025) to ensure consistency. However, analysis results were sensitive to the approach used to account for two "supergroups" of belugas (277 and ≈ 500 whales) encountered outside of transect boundaries and/or off of survey effort. These two whale groups, both encountered near Scammon Bay, Alaska, were an order of magnitude higher than any other group encountered within transect boundaries during this survey (range: 1-38; mean 3). Ignoring these supergroups produced an ensemble estimate of $\widehat{N} = 6{,}360$ (CV 0.16); assuming that all supergroups were detected with certainty (i.e., none were missed within the study area, even outside of surveyed transects) produced an estimate $\widehat{N} = 7{,}917$ (CV 0.13); and treating them as if they had been detected "on effort" resulted in an estimate of $\widehat{N} = 10{,}425$ (CV 0.25). Note that the last estimate was primarily conducted to examine sensitivity of estimates to whether supergroups were detected on or off effort; we do not recommend this estimate for use as distance sampling assumptions are clearly violated. Given the options, we propose the $\widehat{N} = 7{,}917$ (CV 0.13) estimate should be considered as the most justified, though we remain cautious that our estimate could be conservative as missing additional supergroups would have biased this estimate low.

Our DSM estimates were substantially lower than a design-based, stratified estimator fitted to the same data, which produced an estimate of $\widehat{N} = 10{,}966$ (CV 0.30) belugas within the full survey area. However, we caution against using this estimator

because the 2024 surveys were not explicitly design-based. In particular, there was considerable duplicated effort in the 2024 survey, which was primarily concentrated in areas of high beluga density. As such, we would *a priori* expect the design-based estimator to produce a positively biased abundance estimate. However, note that the two beluga supergroups did not contribute to the design-based estimate.

The 2024 estimate of $\widehat{N} = 7{,}917$ (CV 0.13) is considerably smaller than those obtained from spatial analysis of line-transect data in 2017 and 2022, which produced ensemble estimates of $\widehat{N} = 11{,}654$ (CV 0.12) and $\widehat{N} = 13{,}313$ (CV 0.22), respectively (Ferguson et al. 2025), but it is somewhat higher than the estimate of $\widehat{N} = 6{,}994$ produced for surveys in 2000 (Lowry et al. 2017). Part of the reason for this difference may have to do with missed supergroups; for example, our sensitivity analysis produced DSM estimates ranging from 7,842 to 13,042 had we been fortunate enough to observe the supergroups within the transect strip during official survey effort. Owing to this large variability, we are reluctant to conclude that the lower estimate in 2024 relative to 2017 and 2022 is because of a population decline, although we certainly cannot rule this out. Of the existing estimates, the 2022 estimate is likely the most reliable, given that 2022 data better conformed to distance sampling assumptions than sightings in 2024. The 2022 survey also covered a larger area than previous surveys in 2000 and 2017 that may have missed some belugas (Fig. 4).

The presence of supergroups continues a trend first observed in 2022 surveys, where three large groups of belugas (67, 87, 120) were detected north of Scammon Bay. These large groups were largely implicated in the high variability of DSM estimates in analyses of 2022 surveys (Ferguson et al. 2025). By contrast, in 2017, the survey area did

not extend as far south where the large groups were sighted in 2022 and 2024. No large groups were observed in 2017 surveys and the design-based estimator and all DSM models produced similar estimates. Contemporary distance sampling methods seem ill equipped to handle such large variability in group size, and if such trends continue, some other inferential approach will be needed. One such approach is to institute a traditional line-transect design for areas where small groups of whales are typical, with additional effort (e.g., closer transect spacing) in areas where supergroups are expected, to ensure that none are missed. Of course, this assumes that investigators are able to accurately determine where supergroups will be located ahead of time, which would be problematic if such large aggregations form in other locations. Alternatively, some sort of adaptive survey design (*sensu* Thompson 2012) could be considered.

In addition, or perhaps even related to the discussion of supergroups, is an additional novel occurrence observed during 2024 surveys: the presence of killer whales within the EBS survey area. Specifically, a pod of 6 killer whales was observed on 24 June northeast of Pastol Bay, Alaska (Fig. 5), four days prior to the 30 June supergroup sightings to the south. Anecdotally, observers noted that belugas seemed less prevalent in this area when killer whales were present. If the presence of killer whales initiated movement and/or dispersal of belugas out of or within the study area, this would be a violation of basic distance sampling assumptions. This seems likely given reports that monodontids such as belugas often disperse away from killer whales into nearshore, shallow habitat (Shelden et al. 2003, Laidre et al. 2006, Ferguson et al. 2012). It seems likely that highly turbid waters near the Yukon River Delta (including north of Scammon Bay where "supergroups" were encountered) would provide some level of refugia for belugas. Such

movement within the EBS study area could potentially be accounted for using species redistribution models (Conn et al. 2015, Boyd et al. 2018), but such models would require substantially more temporal replication of survey tracks than occurred in the 2024 study. Future survey efforts should consider the potential for killer whales to disrupt the "steady state" spatial distribution of EBS belugas while the survey is being conducted.

ACKNOWLEDGMENTS

The 2024 EBS beluga survey would not have been possible without a large number of collaborators and ongoing partnerships. Many thanks to the Alaska Beluga Whale Committee (ABWC), particularly Tom Gray, Kathy Frost, and John Citta, and the beluga hunters for their dedicated partnership with NMFS to better understand belugas in Alaska through continued research, and to effectively manage the stocks so that they will continue to be available to current and future generations. We would also like to thank pilots Andrew Harcombe and Brian Gieselman; the dispatchers at the U.S. Department of Interior, Bureau of Land Management, Alaska Interagency Coordination Center, South Zone Dispatch; John Bengtson, Robyn Angliss, and leadership at the Alaska Fisheries Science Center and the Marine Mammal Laboratory; the North Slope Borough Department of Wildlife Management; and NOAA grants manager Kristin Cieciel. Funding sources included monies provided by NOAA under the Inflation Reduction Act, by ABWC through a NOAA co-management grant, and the Cooperative Institute for Climate, Ocean, & Ecosystem Studies through NOAA Cooperative Agreement NA20OAR4320271, Contribution No. 2025-1514. Technical reviews of this report were provided by Nancy Young and Alex Zerbini. The findings and conclusions in this paper are those of the author(s) and do not necessarily represent the views of NMFS. Mention of trade names and commercial firms does not imply endorsement by NMFS.

CITATIONS

Adams, M., Frost, K. J., and Harwood, L. A. 1993. Alaska and Inuvialuit Beluga Whale Committee (AIBWC)—An Initiative in" At Home Management". Arctic, 46:134-137.

Bakka, H., Vanhatalo, J., Illian, J. B., Simpson, D., and Rue, H. 2019. Non-stationary Gaussian models with physical barriers. Spatial Statistics, 29:268–288.

Boyd, C., Barlow, J., Becker, E. A., Forney, K. A., Gerrodette, T., Moore, J. E., and Punt, A. E. 2018. Estimation of population size and trends for highly mobile species with dynamic spatial distributions. Diversity and Distributions, 24:1–12.

Buckland, S., Anderson, D., Burnham, K., Laake, J., Borchers, D., and Thomas, L. 2001. Introduction to Distance Sampling: Estimating the Abundance of Biological Populations. Oxford University Press, Oxford, U.K.

Burnham, K. P. and Anderson, D. R. 2002. Model Selection and Multimodel Inference: a Practical Information-theoretic Approach, 2nd Edition. Springer-Verlag, New York.

Citta, J. J., Richard, P., Lowry, L. F., O'Corry-Crowe, G., Marcoux, M., Suydam, R., Quakenbush, L. T., Hobbs, R. C., Litovka, D. I., Frost, K. J., Gray, T., Orr, J., Tinker, B., Aderman, H., and Druckenmiller, M. L. 2017. Satellite telemetry reveals population specific winter ranges of beluga whales in the Bering Sea. Marine Mammal Science, 33:236–250.

Clarke, J. T., Brower, A. A., Ferguson, M. C. and Willoughby, A. L. 2019. Distribution and relative abundance of marine mammals in the Eastern Chukchi and Western Beaufort Seas, 2018. Annual Report, OCS Study BOEM 2019-021. 451 p.

Clarke, J. T., Brower, A. A., Ferguson, M. C., Willoughby, A. L., and Rotrock, A. D. 2020. Distribution and relative abundance of marine mammals in the Eastern Chukchi Sea, Eastern and Western Beaufort Sea, and Amundsen Gulf, 2019. Annual Report, OCS Study BOEM 2020-027. 603 p.

Conn, P.B., and Ferguson, M. C. In review. Correlation between density and detection processes induces bias in spatial models of animal abundance. Environmetrics.

Conn, P. B., Johnson, D. S., Hoef, J. M. V., Hooten, M. B., London, J. M., and Boveng, P. L. 2015. Using spatiotemporal statistical models to estimate animal abundance and infer ecological dynamics from survey counts. Ecological Monographs, 85:235-252.

Conn, P. B., Thorson, J. T., and Johnson, D. S. 2017. Confronting preferential sampling when analysing population distributions: diagnosis and model-based triage. Methods in Ecology and Evolution, 8:1535–1546.

Dunn, P. K. and Smyth, G. K. 2005. Series evaluation of Tweedie exponential dispersion model densities. Statistics and Computing, 15:267–280.

Ferguson, M., Brower, A., Willoughby, A., and Sims, C. 2023. Distribution and estimated abundance of eastern Bering Sea belugas from aerial line-transect surveys in 2017. U.S. Department of Commerce, NOAA Technical Memorandum NMFS-AFSC-471. Available from https://repository.library.noaa.gov/view/noaa/51079. Accessed 26 June 2025.

Ferguson, M. C., Conn, P. B., and Thorson, J. T. 2025. Spatially explicit models of density improve estimates of Easter Bering Sea beluga (*Delphinapterus leucas*) abundance and distribution from line-transect surveys. PeerJ, 13:e20077.

Ferguson S. H., Higdon J. W., and Westdal K. H. 2012. Prey items and predation behavior of killer whales (*Orcinus orca*) in Nunavut, Canada based on Inuit hunter interviews. Aquatic Biosystems, 8:1–16.

Frost, K. J., Gray, T., Goodwin Sr, W., Schaeffer, R., and Suydam, R. 2021. Alaska Beluga Whale Committee—a unique model of co-management. Polar Research, 40:S1.

Hartig, F. 2022. DHARMa: Residual Diagnostics for Hierarchical (Multi-Level / Mixed) Regression Models. R package version 0.4.6.

Hedley, S. and Buckland, S. 2004. Spatial models for line-transect sampling. Journal of Agricultural, Biological, and Environmental Statistics, 9:181–199.

Kristensen, K., Nielsen, A., Berg, C. W., Skaug, H., and Bell, B. M. 2015. TMB: Automatic differentiation and Laplace approximation. Journal of Statistical Software, 70:10.18637/jss.v070.i05.

Laake, J., Miller, D., and Petersma, F. 2024. mrds: Mark-Recapture Distance Sampling. R package version 3.0.0, https://CRAN.R-project.org/package=mrds.

Laidre K. L., Heide-Jorgensen M. P., and Orr, J. R. 2006. Reactions of narwhals, *Monodon monoceros*, to killer whale, *Orcinus orca*, attacks in the eastern Canadian Arctic. Canadian Field Naturalist, 120:457-465.

Lindgren, F., Rue, H., and Lindstrom, J. 2011. An explicit link between Gaussian fields and Gaussian Markov random fields: the stochastic partial differential equation approach. Journal of the Royal Statistical Society B, 73:423–498.

Lowry, L. F., Kingsley, M. C., Hauser, D. D., Clarke, J., and Suydam, R. 2017. Aerial survey estimates of abundance of the eastern Chukchi Sea stock of beluga whales (*Delphinapterus leucas*) in 2012. Arctic, 70:273–286.

Marques, F. F., and Buckland, S. T. 2003. Incorporating covariates into standard line-transect analyses. Biometrics, 59:924–935.

Marsh, H. and Sinclair, D. 1989. Correcting for visibility bias in strip transect aerial surveys of aquatic fauna. Journal of Wildlife Management, 53:1017–1024.

McLaren, I. A. 1961. Methods of determining the numbers and availability of ringed seals in the eastern Canadian Arctic. Arctic, 14:162–175.

Miller, D. L. and Wood, S. N. 2014. Finite area smoothing with generalized distance splines. Environmental and Ecological Statistics, 21:715–731.

Miller, D. L., Burt, M. L., Rexstad, E. A., and Thomas, L. 2013. Spatial models for distance sampling data: recent developments and future directions. Methods in Ecology and Evolution, 4:1001–1010.

O'Corry-Crowe, G. M., Suydam, R. S., Rosenberg, A., Frost, K. J., and Dizon, A. E. 1997. Phylogeography, population structure and dispersal patterns of the beluga whale *Delphinapterus leucas* in the western Nearctic revealed by mitochondrial DNA. Molecular Ecology, 6:955–970.

R Core Team. 2024. R: A Language and Environment for Statistical Computing. R Foundation for Statistical Computing, Vienna, Austria.

Shelden, K. E. W., Brower, A. A., Christman, C. L., and Goetz, K. T. 2024. Distribution of eastern Bering Sea belugas from aerial line-transect surveys in 2024. AFSC Processed Rep. 2024-12, 57 p. Alaska Fish. Sci. Cent., NOAA, Natl. Mar. Fish. Serv., 7600 Sand Point Way NE, Seattle WA 98115.

Shelden, K. E. W., Rugh, D. J., Mahoney, B. A. and Dahlheim, M. E. 2003. Killer whale predation on belugas in Cook Inlet, Alaska: implications for a depleted population. Marine Mammal Science, 19:529–544.

Sigourney, D. B., Chavez-Rosales, S., Conn, P. B., Garrison, L., Josephson, E., and Palka, D. 2020. Developing and assessing a density surface model in a Bayesian hierarchical framework with a focus on uncertainty: insights from simulations and an application to fin whales (*Balaenoptera physalus*). PeerJ, 8:e8226.

Thompson, S. K. 2012. Sampling. John Wiley & Sons.

Wood, S. N. 2003. Thin plate regression splines. Journal of the Royal Statistical Society Series B: Statistical Methodology, 65:95–114.

Wood, S. N. 2017. P-splines with derivative based penalties and tensor product smoothing of unevenly distributed data. Statistics and Computing, 27:985–989.

Wood, S. N., Bravington, M. V., and Hedley, S. L. 2008. Soap film smoothing. Journal of the Royal Statistical Society Series B: Statistical Methodology, 70:931–955.

U.S. Secretary of Commerce
Howard Lutnick

Under Secretary of Commerce
for Oceans and Atmosphere and
NOAA Administrator
Neil Jacobs

Assistant Administrator, National
Marine Fisheries Service.
Eugenio Piñeiro Soler

February 2026

www.nmfs.noaa.gov

OFFICIAL BUSINESS

National Marine
Fisheries Service
Alaska Fisheries Science Center
7600 Sand Point Way N.E.
Seattle, WA 98115-6349